

Fluorescence Modulation by Absorbent on Solid Surface: An Improved Approach for Designing Fluorescent Sensor

*Sheng Yang,[†] Changyao Wang,[†] Changhui Liu, Yijun Wang, Yue Xiao, Jishan Li, Yinhui Li,
and Ronghua Yang**

State Key Laboratory of Chemo/Biosensing and Chemometrics, College of Chemistry and Chemical Engineering, and Collaborative Innovation Center for Chemistry and Molecular Medicine, Hunan University, Changsha, 410082, China.

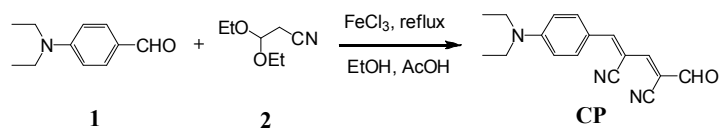
[†]These authors contributed equally

* To whom correspondence should be addressed

E-mail: Yangrh@pku.edu.cn

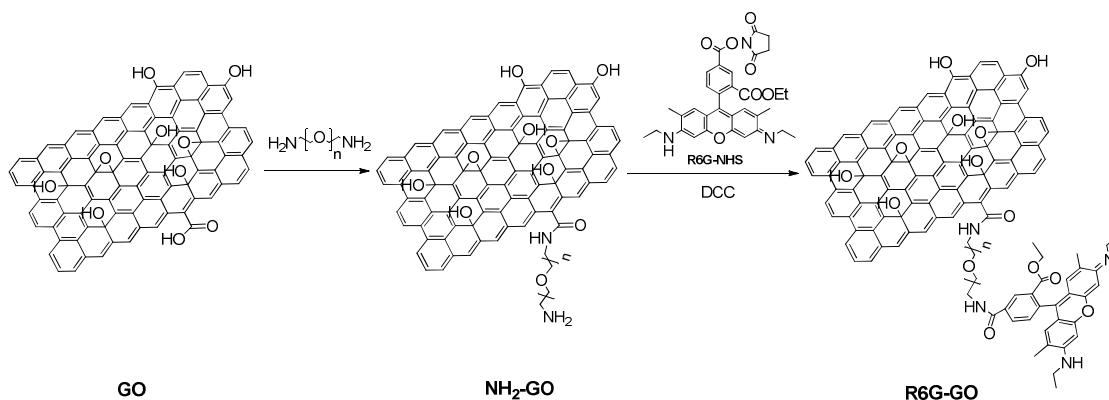
Fax: +86-731-88822523

1. SYNTHESIS



Scheme S1. Synthetic route of **CP**.

Synthesis of CP. The starting material **1** and **2** are commercially available. $\text{FeCl}_3 \cdot 6\text{H}_2\text{O}$ (14.31 mg, 0.05 mmol) was added to a solution of 4-(diethylamino)benzaldehyde **1** (37.2 mg, 0.21 mmol) and 3,3-diethoxypropanenitrile **2** (60.1 mg, 0.42 mmol) in ethanol/acetic acid (2 ml, v/v = 1:5), and the reaction mixture was then stirred at 90 °C for 5 h. Subsequently, the solvent was removed under reduced pressure and the crude product was purified by chromatography on a silica gel column with a mixture of ethyl acetate/ petroleum ether (5: 1, v/ v) as the mobile phase, affording compound **CP** as a brown solid (10.5 mg, 17.9%). ^1H NMR (400 MHz, CDCl_3): δ = 9.48 (s, 1H), 7.96 (d, J = 8.8, 3H), 7.67 (s, 1H), 6.80 (d, J = 8.8, 2H), 3.51 (dd, J = 7.2, 2H); MS ($M^+ + 1$): 279.34.



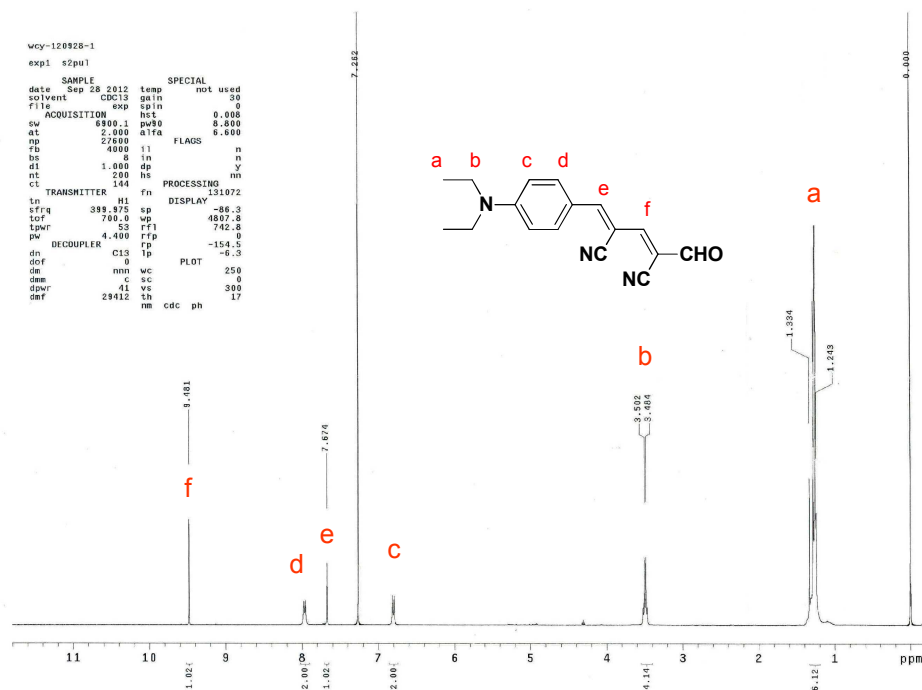
Scheme S2. Synthetic route of **R6G-GO**.

Synthesis of R6G-GO. GO was refluxed in SOCl_2 (20 mL) in the presence of DMF (0.5 mL) at 70 °C for 24 h under argon atmosphere, which could lead to the chloroformylation of carboxyl groups on GO. The reaction mixture was centrifuged, and the supernatant was decanted. The residue was washed three times with anhydrous tetrahydrofuran, followed by

drying in vacuum at room temperature. In the presence of triethylamine (Et_3N , 0.5mL), the obtained chloroformylated GO was dispersed in dichloromethane, and then added dropwise to the dichloromethane solution of 1,11-Diamino-3,6,9-trioxaundecane (5mg). The reaction mixture was stirred at room temperature for 4 h. After centrifugation, the supernatant was discarded and the residue was washed three times with dichloromethane. Then, the residue was dried under N_2 gas, yielding the amino-coated GO (abbreviated as **NH₂-GO**). To the suspension of **NH₂-GO** in DMF, 5-Carboxyrhodamine 6G succinimidyl ester (R6G-NHS, 5 mg) and DCC were added. After stirring for 24 h at room temperature, the reaction mixture was centrifuged, and the residue was further purified by washing several times with water until the supernatant was almost colorless. The product was then washed with a small quantity of H_2O to remove Et_3NHCl , and finally dried under vacuum to yield the **R6G-GO**.

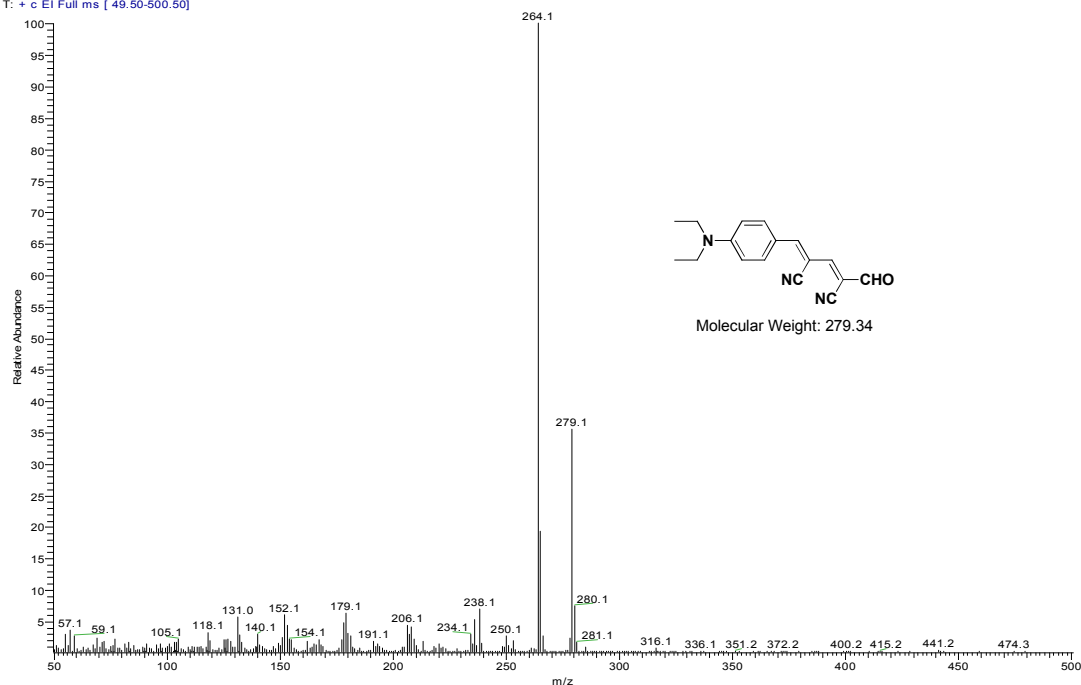
2. NMR and Mass Spectra of compound CP.

^1H NMR of compound **CP** in CDCl_3



EI-MS of compound **CP**

ysh-120509-228 #22 RT: 3.81 AV: 1 NL: 3.67E6
T: + c EI Full ms [49.50-500.50]



3. SPECTROSCOPIC DATA

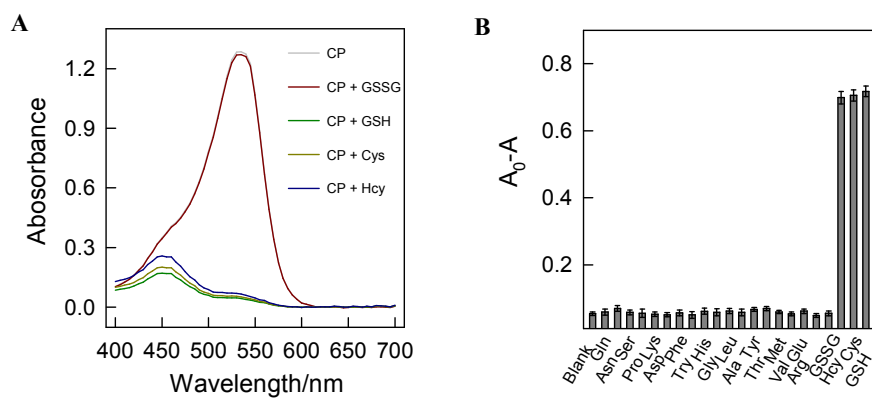


Figure S1. (A) Absorption spectra of 200 μM **CP** in HEPES buffer solution (pH 7.4) in the absence and presence of 10 mM GSSG, GSH, Cys, Hcy, respectively. (B) Absorption changes ($A_0 - A$) of 200 μM **CP** in the presence of 1 mM various amino acids without thiol groups, secondary thiol, and biothiols. All error bars were obtained through the detection of three parallel samples.

wchy-140317-586-1-#3 RT: 0.13 AV: 1 NL: 3.27E5
T: + c ESI ms [50.00-1500.00]

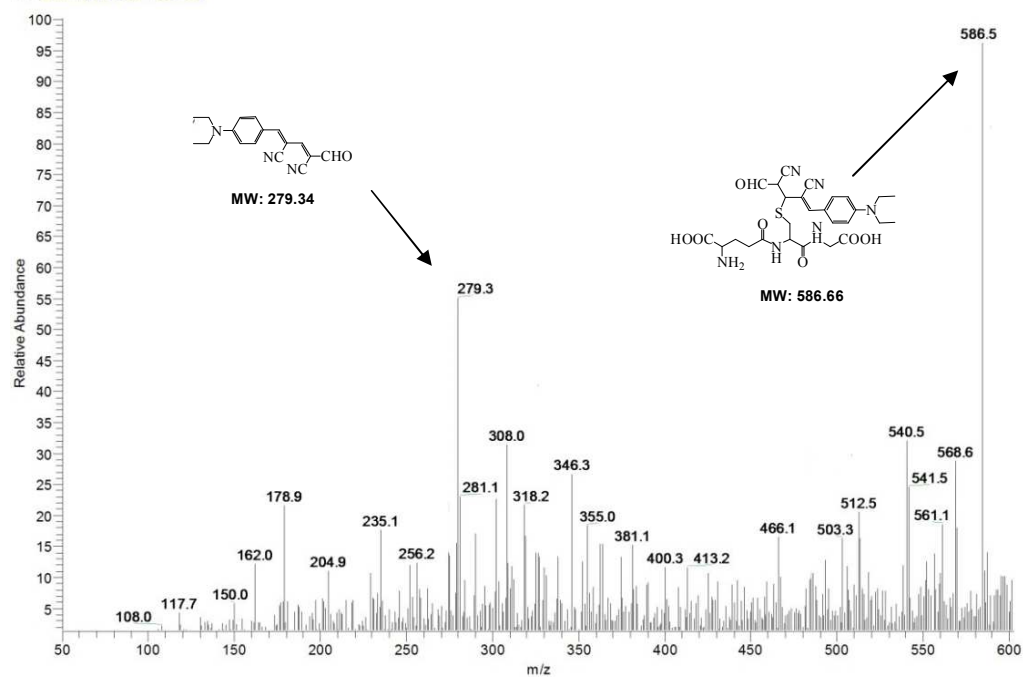


Figure S2. ESI-MS of the reaction of CP and GSH.

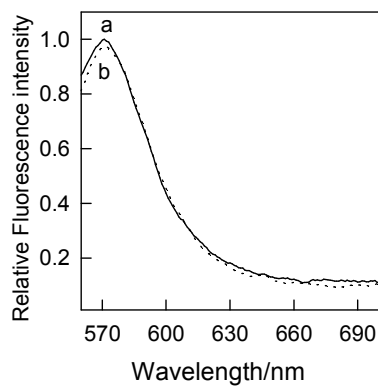


Figure S3. Fluorescence emission spectra ($\lambda_{\text{ex}} = 537$ nm) of 1.0 μ M R6G in the absence (a) and presence (b) of 40 mM GSH.

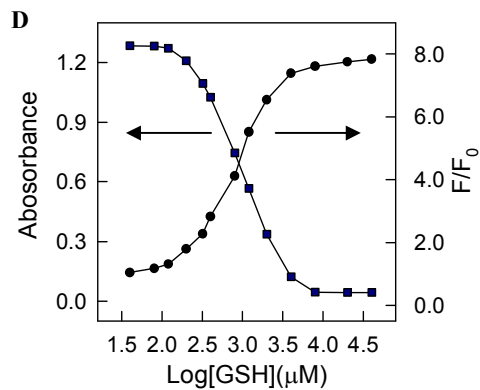


Figure S4. Comparison of absorptiometric and fluorometric techniques for GSH detection.

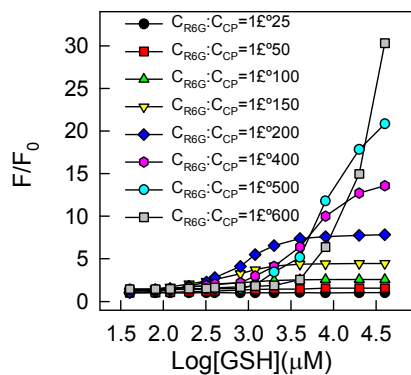


Figure S5. Effects of different composition ratios of R6G and CP on the fluorescence responses to different concentrations of GSH. $[R6G] = 1 \mu M$, $[CP] = 25\text{--}200 \mu M$, $[GSH] = 0\text{--}40 \text{ mM}$. $\lambda_{ex}/\lambda_{em} = 537 \text{ nm}/571 \text{ nm}$.

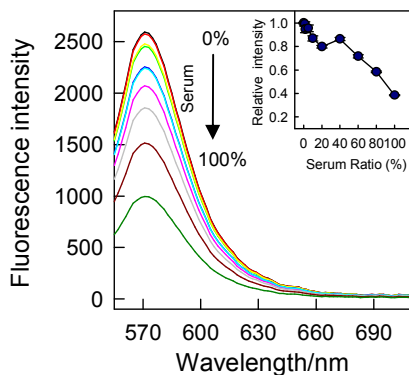


Figure S6. Fluorescence emission changes of $1.0 \mu M$ R6G in the presence of different ratio of serum to buffer solution (0-100%). All error bars were obtained through the detection of three parallel samples. $\lambda_{ex}/\lambda_{em} = 537 \text{ nm}/571 \text{ nm}$.

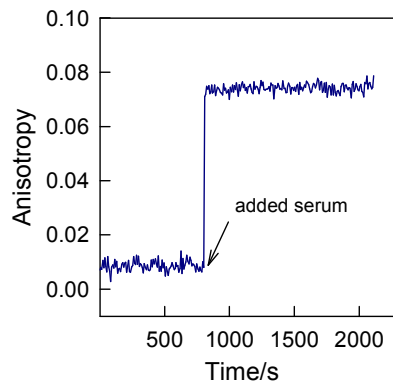


Figure S7. Real-time FA records of R6G in buffer solution (50% ethanol, pH 7.4) upon addition of 50% bovine serum samples.

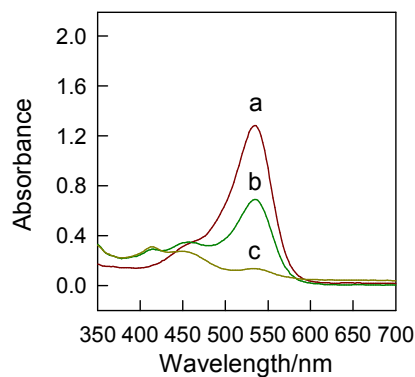


Figure S8. UV-vis absorbance spectra of CP (a), CP + 20 % bovine serum (b), and CP + 20 % bovine serum + GSH (c) in HEPES buffer solution . [CP] = 200 μ M, [GSH] = 10 mM.

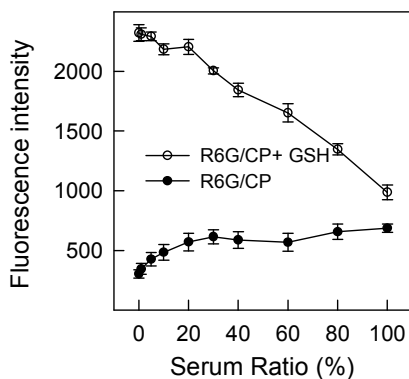


Figure S9. Fluorescence emission changes of R6G/CP ([R6G] = 1 μ M, [CP] = 200 μ M) in the absence and presence of 40 mM GSH with different ratio of serum to buffer solution (0-100%) All error bars were obtained through the detection of three parallel samples. $\lambda_{\text{ex}}/\lambda_{\text{em}}$

= 537 nm/571nm.

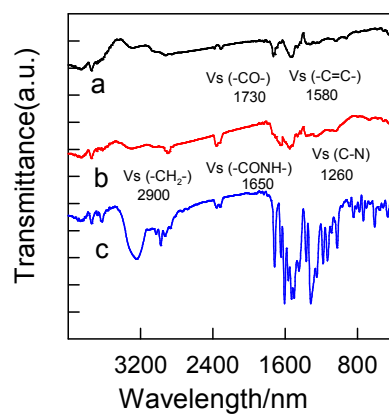


Figure S10. FTIR spectroscopy of GO (a), **R6G-GO** (b), and R6G (c).

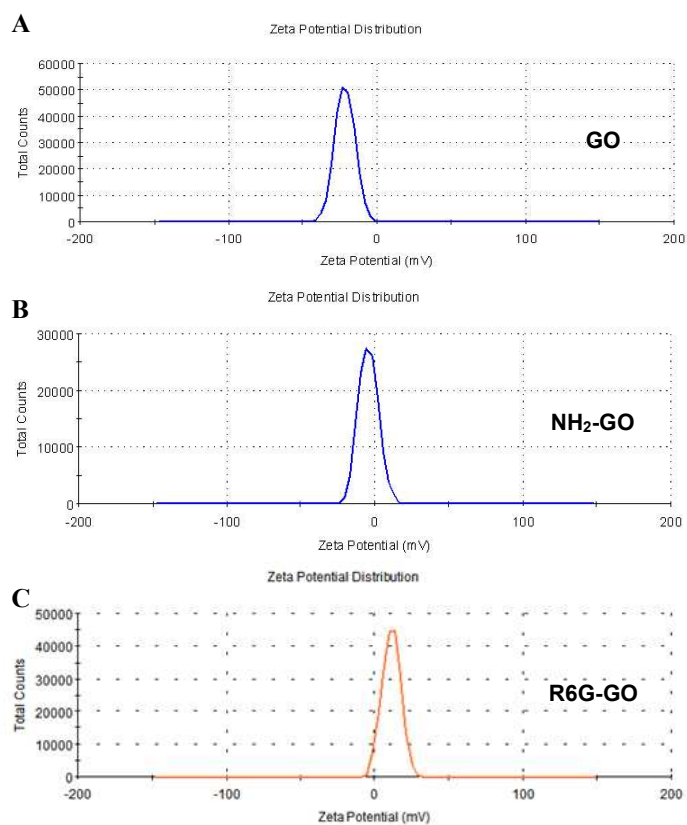


Figure S11. FTIR spectroscopy of GO (a), **$\text{NH}_2\text{-GO}$** (b), and **R6G-GO** (c).

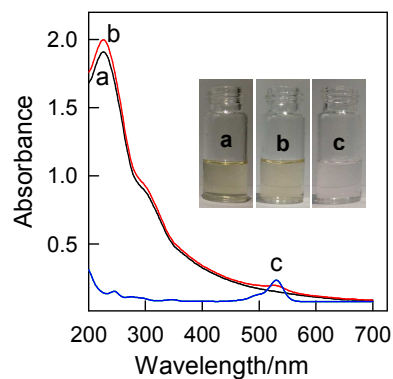


Figure S12. UV-vis absorbance spectra of GO (a), **R6G-GO** (b) , and R6G (c) in HEPES buffer solution (pH 7.4). Inset: photographs show the corresponding color.

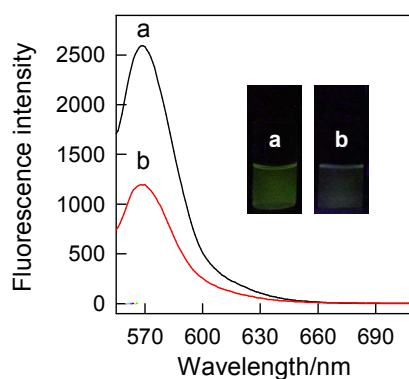


Figure S13. Fluorescence spectra of 1 μM R6G (a) and 40 $\mu\text{g/mL}$ **R6G-GO** (b) in HEPES buffer solution (pH 7.4). Inset: photographs show the corresponding fluorescent color illuminated with a hand-held UV lamp (365nm). $\lambda_{\text{ex}}/\lambda_{\text{em}} = 537 \text{ nm}/571 \text{ nm}$.

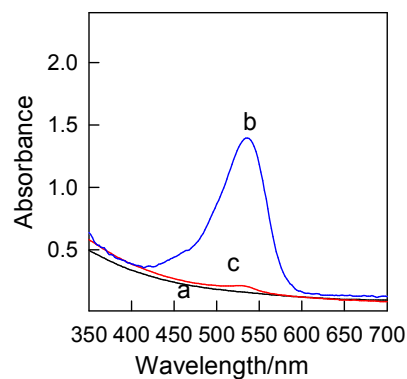


Figure S14. UV-vis absorbance spectra of GO (a), **R6G-GO /CP** (b), and **R6G-GO /CP +**

GSH (c) in HEPES buffer solution (pH 7.4). [GO] = 40 $\mu\text{g/mL}$, [CP] = 200 μM , [R6G] = 1 μM , [GSH] = 10 mM.

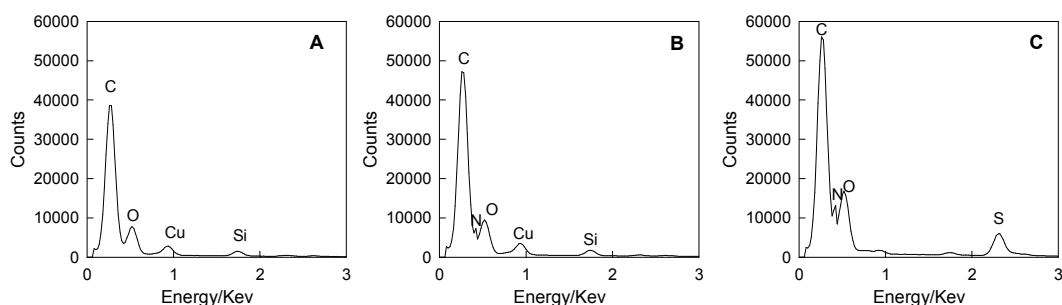


Figure S15. EDX data of GO (A), R6G-GO /CP (B), and R6G-GO /CP + GSH (C).

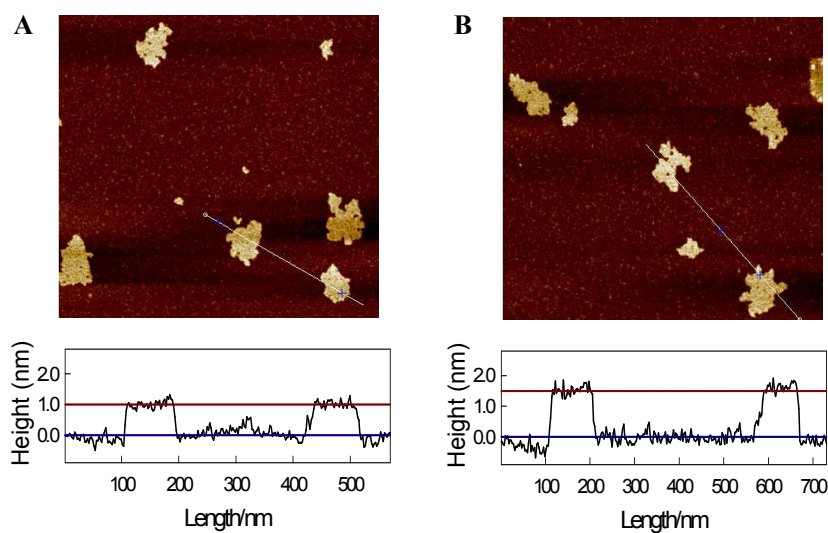


Figure S16. Tapping-mode AFM images and line profile of GO (A) and R6G-GO /CP nanocomposites (B).

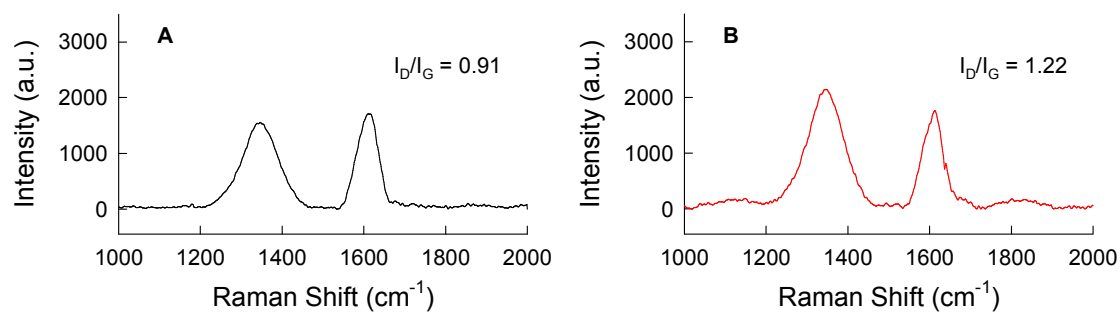


Figure S17. The Raman spectra of (A) GO and (B) R6G-GO /CP.

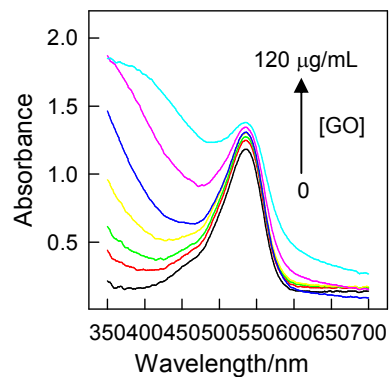


Figure S18. Absorption spectra of 200 μM CP towards different concentrations of GO (0-120 $\mu\text{g/mL}$) in HEPES buffer solution (pH 7.4).

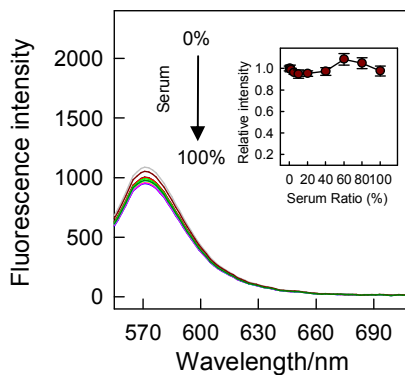


Figure S19. Fluorescence emission changes of 40 $\mu\text{g/mL}$ R6G-GO in the presence of different ratio of serum to buffer solution (0-100%). $\lambda_{\text{ex}}/\lambda_{\text{em}} = 537 \text{ nm}/571 \text{ nm}$.

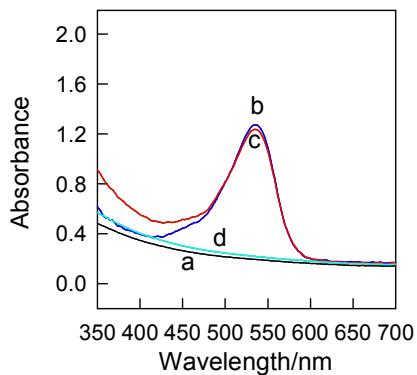


Figure S20. UV-vis absorbance spectra of GO (a), GO /CP (b), GO /CP + 20 % bovine serum (c), and GO /CP + 20 % bovine serum + GSH (d) in HEPES buffer solution . $[\text{GO}] = 40 \mu\text{g/mL}$, $[\text{CP}] = 200 \mu\text{M}$, $[\text{GSH}] = 10 \text{ mM}$.

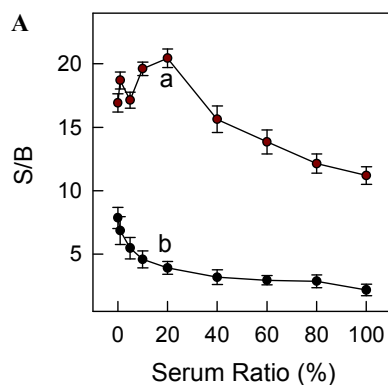


Figure S21. *S/B* ratios of **R6G-GO/CP** (a) and **R6G/CP** (b) response toward GSH as a function of the ratio of bovine serum to buffer solution. [R6G-GO] = 40 $\mu\text{g/mL}$, [R6G] = 1 μM , [CP] = 200 μM , [GSH] = 40 mM. All error bars were obtained through the detection of three parallel samples. $\lambda_{\text{ex}}/\lambda_{\text{em}} = 537 \text{ nm}/571 \text{ nm}$.

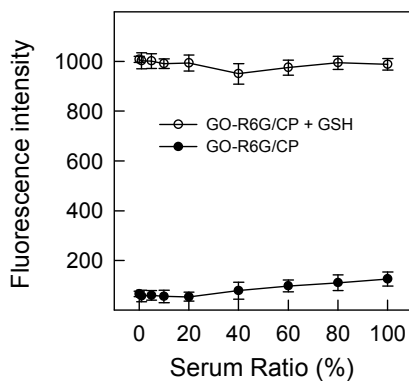


Figure S22. Fluorescence emission changes of **R6G-GO/CP** ([R6G-GO] = 40 $\mu\text{g/mL}$, [CP] = 200 μM) in the absence and presence of 40 mM GSH with different ratio of serum to buffer solution (0-100%) All error bars were obtained through the detection of three parallel samples. $\lambda_{\text{ex}}/\lambda_{\text{em}} = 537 \text{ nm}/571 \text{ nm}$.

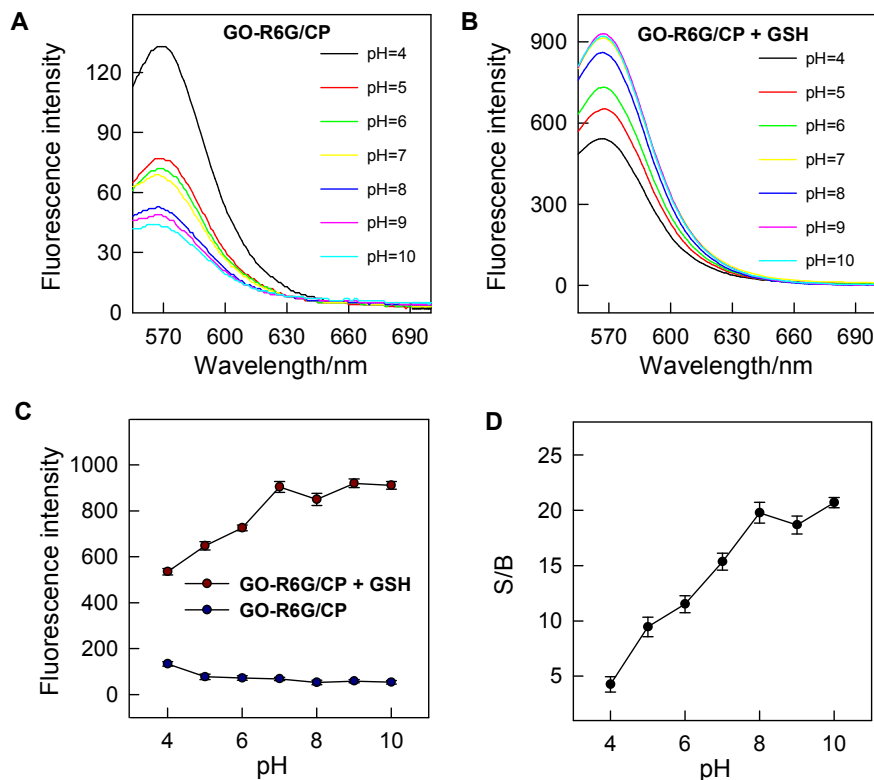


Figure S23. Fluorescence emission spectra of **R6G-GO/CP** ($[R6G-GO] = 40 \mu\text{g/mL}$, $[CP] = 200 \mu\text{M}$) in the absence (A) and presence (B) of 40 mM GSH in 20% bovine serum solution with different pH (4-10) and the corresponding intensity changes (C) and signal to background ratios (D) as a function of pH changes. $\lambda_{\text{ex}}/\lambda_{\text{em}} = 537 \text{ nm}/571 \text{ nm}$.

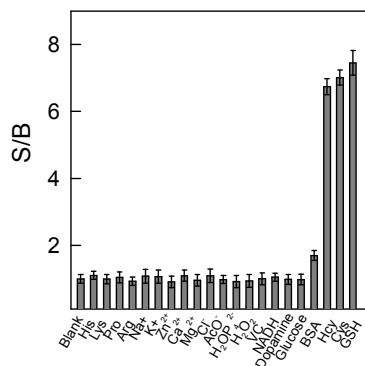


Figure S24. Signal to background ratios (S/B) of **R6G-GO/CP** ($[R6G-GO] = 40 \mu\text{g/mL}$, $[CP] = 200 \mu\text{M}$) response toward 1 mM various biologically relevant species in buffer solution with 20 % bovine serum. All error bars were obtained through the detection of three parallel samples.

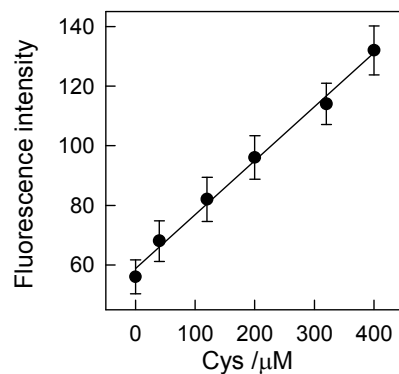


Figure S25. linear responses of fluorescence intensity of **R6G-GO/CP** ($[R6G-GO] = 40 \mu\text{g/mL}$, $[CP] = 200 \mu\text{M}$) to changing Cys concentrations (0-400 μM) in buffer solution with 20 % human serum (pH 7.4). All error bars were obtained through the detection of three parallel samples. $\lambda_{\text{ex}}/\lambda_{\text{em}} = 537 \text{ nm}/571\text{nm}$.

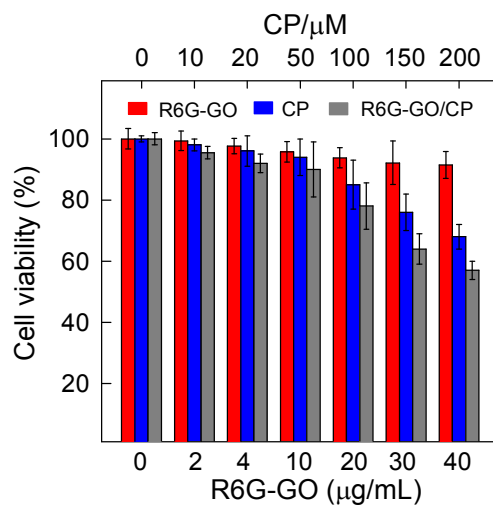


Figure S26. Cell viability of HeLa treated with different concentration of R6G-GO, CP, and R6G-GO/CP for 24 h in fresh medium.

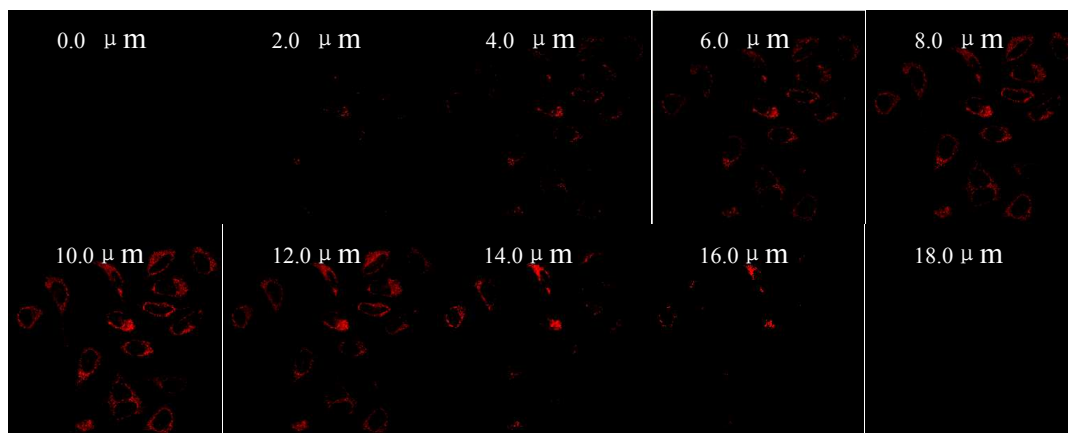


Figure S27. Z-scanning confocal fluorescence microscopy images of HeLa cells incubated with R6G-GO/CP.

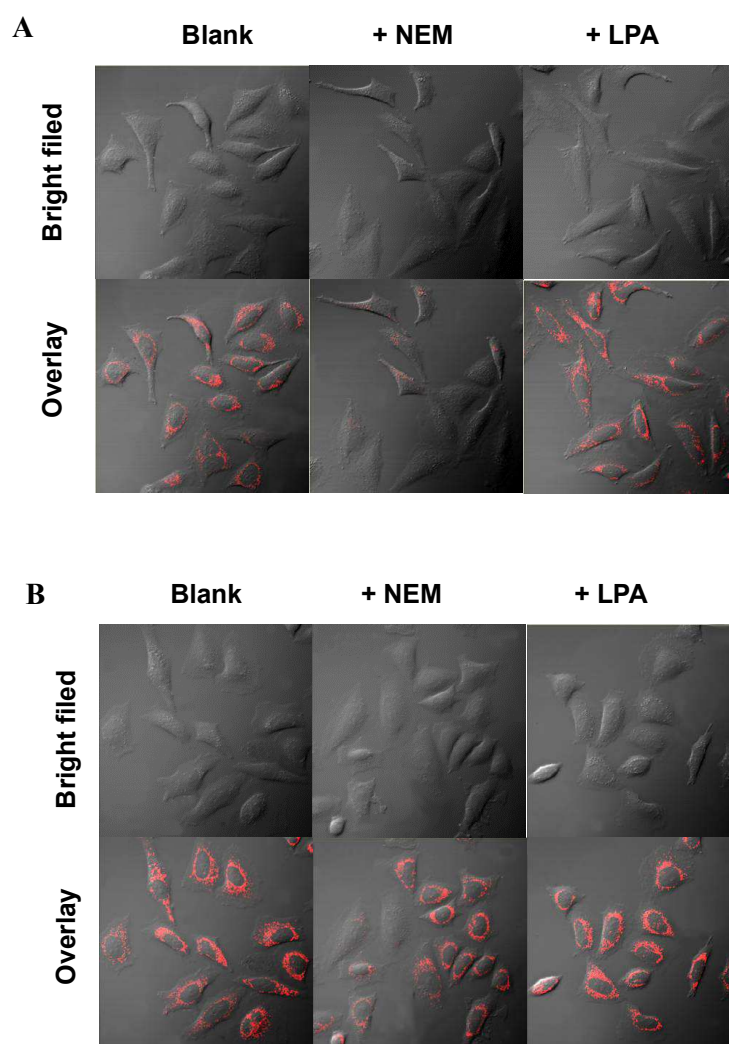


Figure S28. Bright-field images (up) and the overlay of fluorescence and bright-field images(down) of HeLa cells using **R6G-GO/CP** (A) and **R6G/CP** (B) under different conditions. (left) untreated. (middle) pretreated with NEM (500 μ M) for 40min. (right) pretreated with LPA (500 μ M) for 12h.